Dalton Transactions

ROYAL SOCIETY OF CHEMISTRY

PAPER

View Article Online
View Journal

Cite this: DOI: 10.1039/d6dt00599c

Niobium oxyiodide clusters from heterogeneous solid-state reactions: the example of $Li_3Nb_7O_5I_{14}(NbI_6)$

Jan Beitlberger, Patrick Schmidt and H.-Jürgen Meyer *

Received 11th March 2026,
Accepted 13th April 2026

DOI: 10.1039/d6dt00599c

rsc.li/dalton

No fewer than nine niobium oxyiodide phases have been synthesised and characterised from the reaction between NbI_4 and Li_2O in the presence of $Li_2(CN_2)$ under closed-system conditions at temperatures between 400 °C and 500 °C. Reactions in this system proceed through diffusion-controlled solid–solid pathways as well as gas-phase reactions that extend beyond equilibrium, which enables the concurrent formation of multiple niobium oxyiodide compounds. The crystal structures of these products display a range of architectures based on different niobium oxide clusters, including the $[Nb_7O_5]$ core, which is a characteristic structural motif in the structure of $Li_3Nb_7O_5I_{14}(NbI_6)$, the compound examined in this report.

Introduction

Metal-rich halide cluster compounds of group 5 and 6 transition metals are well known. Among binary niobium iodides, well known representatives are Nb_6I_{11}, Nb_3I_8, NbI_3, and NbI_4.[1–3] These compounds are typically synthesised through metallothermic reactions involving binary metal halides. For example, Nb_6I_{11} is commonly prepared from Nb_3I_8 and metallic niobium at elevated temperatures,[1] whereas Nb_3I_8 itself is obtained from reactions between niobium powder and niobium pentaiodide.[2]

The extension of the metal-rich systems with chalcogenide or pnictide anions has greatly broadened this chemistry, leading to the formation of numerous heteroanionic cluster compounds. These compounds can be regarded as architectures in which anions are either substituted or structurally integrated, often necessitating distinct coordination environments. Variations in connectivity and structural motifs are evident, for example, in the structures of one-dimensional compounds such as Nb_6I_9S and ANb_3Br_7S (A = Rb and Cs).[4] Further structural diversity is observed in chalcogenide-containing compounds such as Nb_3TeI_7,[5] $Nb_4Se_4I_4$,[6] and $Nb_7S_2I_{19}$,[7] as well as in layered pnictide analogues like Nb_4PnX_{11} (Pn = N and P; X = Cl, Br, and I).[8] Beyond differences in the number of Nb atoms constituting the cluster cores, these compounds display pronounced variations in their electronic structures and properties.

Section for Solid State and Theoretical Inorganic Chemistry, Institute of Inorganic Chemistry, Auf der Morgenstelle 18, Eberhard Karls Universität Tübingen, 72076 Tübingen, Germany. E-mail: juergen.meyer@uni-tuebingen.de

Niobium oxyiodides such as $NbOI_3$, NbO_2I, and the metal-rich $NbOI_2$ have been known for a long time and studied intensively.[9] Condensed niobium oxide iodides are highly volatile and can be crystallised only within narrow equilibrium conditions. This highlights the sensitivity of these systems to parameters such as temperature, pressure, and composition, all of which profoundly influence the formation of distinct niobium oxyiodide phases.

The semiconducting compounds $NbOX_2$ (X = Cl, Br, and I) can be synthesised from Nb powder, Nb_2O_5, and NbX_5 and have been studied for applications such as photocatalytic water splitting,[10] 2D dielectric capacitors,[11] and ferroelectric materials.[11,12] Metallothermic reduction remains a conventional and efficient route for preparing $NbOX_2$ and related metal-rich metal halides. An alternative approach, introduced by L. Messerle *et al.*, uses bismuth as a "non-conventional" reducing agent.[13] Additional soft reduction pathways have been reported using transition metals M = Cr, Mn, Fe, Co, or Ni.[14,15] Owing to their lower electropositivity, these reduction agents facilitate the formation of multiple intermediate compounds with progressively decreasing oxidation states, as has been exemplified by the reduction cascade from WCl_6 to WCl_2, which illustrates a distinctive reduction mechanism.[15] Following this mechanism, the reductant metal (M) is first incorporated and then released as MCl_x.

Lithium carbodiimide is known to serve as a reactant delivering $(NCN)^{2-}$ ions in solid-state metathesis (SSM) reactions with metal halides, yielding metal carbodiimides.[16] However, when it is reacted with more electropositive metal halides, $Li_2(CN_2)$ instead acts as a reducing agent. This has been demonstrated by its reaction with $NiCl_2$, which produces

metallic nickel along with C_3N_4.[17] In other combinations, $Li_2(CN_2)$ exhibits only a weaker reducing effect.

Transferring these findings, we explored the Nb–O–I system by reacting NbI_4 with Li_2O in the presence of $Li_2(CN_2)$. Our previous results demonstrated that interactions among NbI_4, Li_2O, and $Li_2(CN_2)$ generate a heterogeneous system in which local temperature and pressure variations strongly affect the phase formation.[18] As a result of these investigations, we have already identified a family of Nb_4O_{12-x} compounds, namely Nb_4OI_{12}, two modifications of Nb_4OI_{11}, and Nb_4OI_{10}, all featuring rectangular $[Nb_4O]$ cluster cores.[19] From the same reaction system, we also obtained $Nb_5O_4I_{11}$ featuring a $[Nb_5O_4]$ cluster core.[20] Subsequent reactions produced $Li_3Nb_7O_5I_{15}$ and $Nb_8O_5I_{17}(NbI_5)$, which contain $[Nb_7O_5]$ and $[Nb_8O_5]$ cluster cores, respectively; the latter is extended by an additional niobium atom.[18] More recently, we reported two new compounds $Nb_6O_3I_{15}$ and $Nb_{11}O_6I_{24}$, forming three-dimensional and one-dimensional assemblies of their crystal structures.[21] The compound presented in this work, $Li_3Nb_7O_5I_{14}(NbI_6)$, is proposed as the competing phase to the formation of $Li_3Nb_7O_5I_{15}$.

Results and discussion

The Nb–O–I system was investigated by reacting NbI_4 with Li_2O in the presence of $Li_2(CN_2)$, loaded into fused silica ampoules. Both the previously reported reactions and the one described here were conducted with minor adjustments to the relative amounts of starting materials. The temperature programs applied to the silica ampoules were varied within narrow limits, while the overall reaction volume was kept constant. A natural temperature gradient along the ampoule was consistently evidenced by the occurrence of small amounts of volatile $NbOI_2$ as a side-phase, which was typically found at the cooler end of the ampoule.

Essentially all niobium oxyiodide compounds discussed in the Introduction section are formed close to 500 °C, appearing in the reaction vessel in different combinations with each other. These compounds occur as crystalline materials, including well-formed single-crystals, distributed across several regions in the silica ampoule. Their spatial distribution highlights the crucial role of gas-phase species in transporting both, reactants and products throughout the system.

Only two compounds, the previously reported $Li_3Nb_7O_5I_{15}$ [18] and the new $Li_3Nb_7O_5I_{14}(NbI_6)$, were obtained at the bottom of the silica ampoule. These compounds are likely formed without the involvement of a gas-phase transport process. In addition, $Li_3Nb_7O_5I_{14}(NbI_6)$ is produced at significantly lower temperatures and appears consistently in all reactions, although in varying quantities. At 450 °C, it is observed as a black, poorly crystalline powder. Unfortunately, the crystallinity and the crystal size of this compound were insufficient to fully characterise the compound by single-crystal X-ray analysis with acceptable refinement values. Therefore, the crystalline powder of $Li_3Nb_7O_5I_{14}(NbI_6)$ was analysed by powder X-ray diffraction, and the crystal structure was refined by Rietveld analysis. The corresponding diffraction pattern showing the final structure refinement is presented in Fig. 1, and relevant refinement parameters are summarised in Table 1.

Overall, this system generates a range of niobium oxyiodides, but these phases are thermally metastable, as evidenced by their transformation into $NbOI_2$ at temperatures exceeding 500 °C.

The structural refinement of the crystalline powder of $Li_3Nb_7O_5I_{14}(NbI_6)$ by means of Rietveld refinement reveals a close relationship with the structure of $Li_3Nb_7O_5I_{15}$. $Li_3Nb_7O_5I_{14}(NbI_6)$ was found to crystallise orthorhombically in the space group *Imma*, featuring four crystallographically distinct niobium sites and three distinct oxygen sites in the structure. The localisation and refinement of lithium ions in the structure was fostered by their presence in special Wyckoff positions 4*e* of Li1 and Li2, and 4*f* of Li3.

The crystal structure of $Li_3Nb_7O_5I_{14}(NbI_6)$ is based on a $[Nb_7O_5]$ cluster core (Fig. 2) that has been previously reported as a basic building block in other crystal structures of niobium oxyiodides, obtained in the same reaction system.[18] The niobium-to-niobium distances within the $[Nb_7O_5]$ cluster core of $Li_3Nb_7O_5I_{14}(NbI_6)$ range between 2.71(1) Å and 3.097(9) Å, which are in good accordance with the corresponding distances in $Li_3Nb_7O_5I_{15}$ (Table 2). This type of cluster core is surrounded by iodine atoms, which can be assigned as inner (i), outer (a), and outer–outer bridging (a–a) ligands when following the nomenclature that has been originally introduced for octahedral cluster compounds.[22]

The surrounding of the cluster core with iodine atoms (Fig. 3) coincides with the pattern obtained in $Li_3Nb_7O_5I_{15}$,[18] with relevant distances summarised in Table 2. Besides four inner I^i and outer I^a, there are twelve surrounding I^{a-a} iodine atoms making up a $[Nb_7O_5I_4{}^iI_4{}^aI_{12/2}{}^{a-a}]$ cluster (Fig. 3) in the structure of $Li_3Nb_7O_5I_{14}(NbI_6)$. The connectivity between adjacent clusters is established by six pairs of I^{a-a} bridges departing from each of the six corners of niobium atoms of the $[Nb_7O_5]$ core, to build up a three-dimensional network, indicated by broken-off bonds in Fig. 3. The connectivity pattern

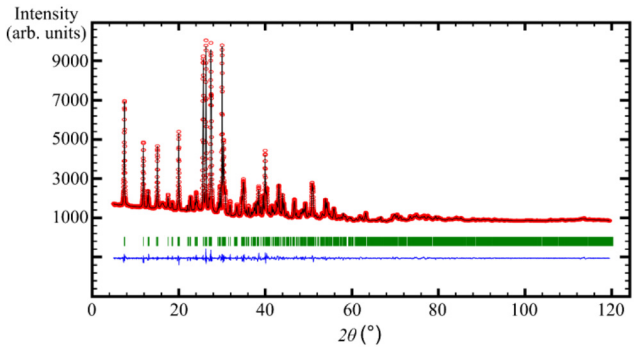

Fig. 1 Powder X-ray diffraction pattern subjected to Rietveld refinement for the crystal structure of $Li_3Nb_7O_5I_{14}(NbI_6)$ at 298 K, with the experimental (red) and calculated (black) intensities, Bragg positions (green), and the difference curve (blue) shown.

Table 1 Selected crystallographic data and Rietveld refinement values of $Li_3Nb_7O_5I_{14}(NbI_6)$

	$Li_3Nb_7O_5I_{14}(NbI_6)$
CCDC	2493985
Crystal system	Orthorhombic
Space group	*Imma*
Temperature (K)	298
Unit cell dimensions (Å)	a = 13.5176(1) b = 13.4466(2) c = 23.7811(3)
Volume (Å^3)	4322.56(9)
Z	4
Wavelength, Cu-K$_\alpha$, (Å)	1.54060
μ (mm^{-1})	128.992
Reflections collected	1856
Parameters	261
R_{Bragg}	2.734
R_p/R_{wp}	3.143/4.2119
X^2	1.3461

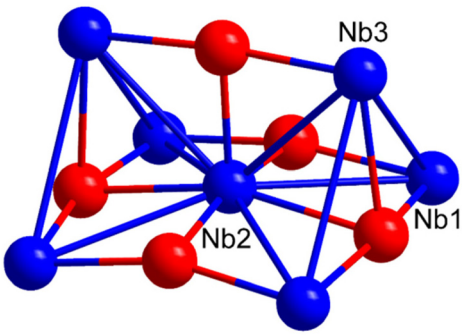

Fig. 2 Structure of the $[Nb_7O_5]$ cluster core inside $Li_3Nb_7O_5I_{14}(NbI_6)$, with labelled niobium atoms.

Table 2 Selected interatomic distances in $Li_3Nb_7O_5I_{14}(NbI_6)$ and $Li_3Nb_7O_5I_{15}$

Distances/Å	$Li_3Nb_7O_5I_{14}(NbI_6)$	$Li_3Nb_7O_5I_{15}$ [18]
Nb1–Nb2	2.821(7)	2.8050(4)
Nb1–Nb3	3.097(9)	3.0667(6)
Nb2–Nb3	2.71(1)	2.7883(7)
Nb–O	1.902(6)–2.254(9)	1.9464(6)–2.247(6)
Nb–I^i	2.825(9)–2.842(5)	2.7528(5)–2.7908(3)
Nb–I^a	2.934(9)	2.8761(5)
Nb–I^{a-a}	2.92(1)–2.994(8)	2.9105(7)–3.0224(5)
Nb–I of $[NbI_6]^-$	Nb4–I4: 2.57(1); Nb4–I6: 2.598(7); Nb4–I7: 2.756(6); Nb4–I8: 3.09(2)	—
Li–I^a	2.722(5)–2.95(2)	2.904(6)–2.97(1)
Li–I^{a-a}	2.750(6)	3.17(1)
Li–I to other iodides	Li1–I4: 2.83(1); Li2–I8: 2.9(3); Li3–I8: 3.218(5)	Li–I5: 2.64(2)–2.76(2)

in this network creates open channels to host molecular $(NbI_6)^-$ units with average Nb–I distances of ~2.73 Å, displayed as a blue polyhedron in Fig. 4. The incorporation of (NbI_5)

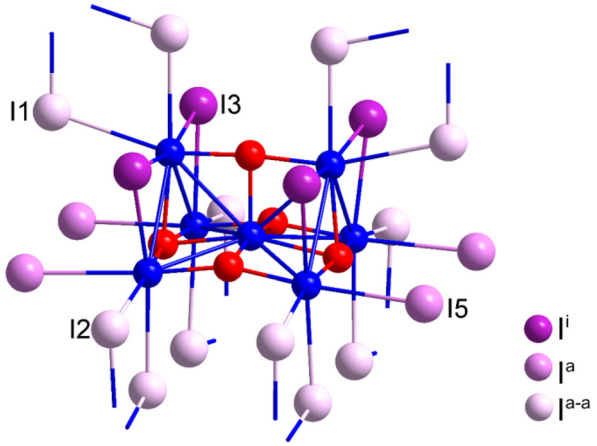

Fig. 3 Iodide coordination of the $[Nb_7O_5]$ cluster core with the connectivity implied by the broken bonds. Niobium atoms are coloured in blue, oxygen in red and iodide in pink.

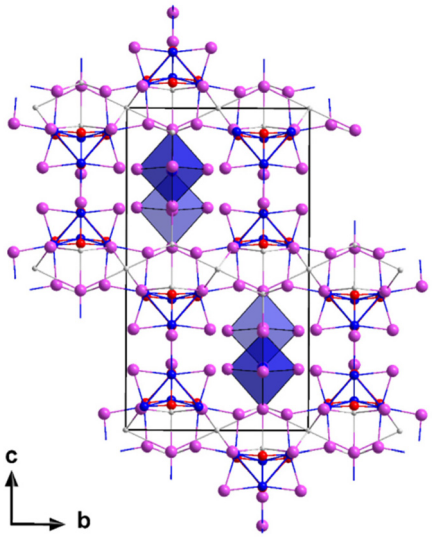

Fig. 4 Section of the crystal structure viewed along the *a*-direction, with $(NbI_6)^-$ units shown as blue octahedra.

molecules has been previously reported in $Nb_8O_5I_{17}(NbI_5)$ with an average Nb–I distance of ~2.66 Å.[18] An example of a $(TaBr_6)^-$ ion is represented in the structure of the octahedral cluster compound $(Ta_6Br_{15})(TaBr_6)_{0.86}$ with an average Ta–Br distance of ~2.53 Å.[23]

Lithium ions in the crystal structure of $Li_3Nb_7O_5I_{14}(NbI_6)$ are refined in nearly square-pyramidal (Li1 and Li2) and distorted octahedral (Li3) iodide environments (Fig. 5). A similar square-pyramidal environment of lithium ions was also observed in the structure of $Li_3Nb_7O_5I_{15}$, here with an average Li–I distance of 2.85 Å. The octahedrally surrounded Li3 atom shows an average Li–I distance of 3.05 Å.

The crystal structure of $Li_3Nb_7O_5I_{14}(NbI_6)$ displays a close resemblance to that of $Li_3Nb_7O_5I_{15}$ when substituting the $(NbI_6)^-$ with one I^- ion. This incorporation of $(NbI_6)^-$ as an

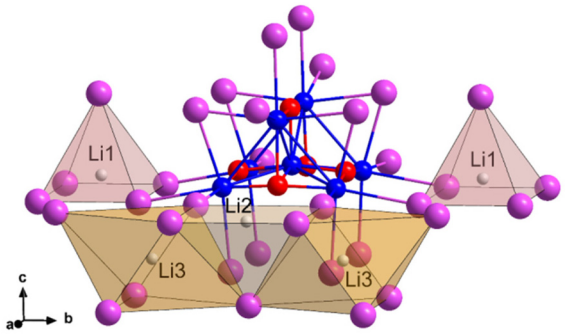

Fig. 5 Iodide coordination of the lithium atoms inside $Li_3Nb_7O_5I_{14}(NbI_6)$.

anion clarifies that $Li_3Nb_7O_5I_{14}(NbI_6)$ can also be described as a double salt, which leads to the formula $Li_2[Nb_7O_5I_{14}]{\cdot}Li[NbI_6]$. In this respect, $Li_3Nb_7O_5I_{15}$ could be as well depicted as $Li_2Nb_7O_5I_{14}{\cdot}LiI$.

In spite of the similarity of local structures and bridging iodine atoms in $Li_3Nb_7O_5I_{15}$ and $Li_3Nb_7O_5I_{14}(NbI_6)$ there are clear differences in the connectivity patterns between clusters in both structures (Fig. 6).

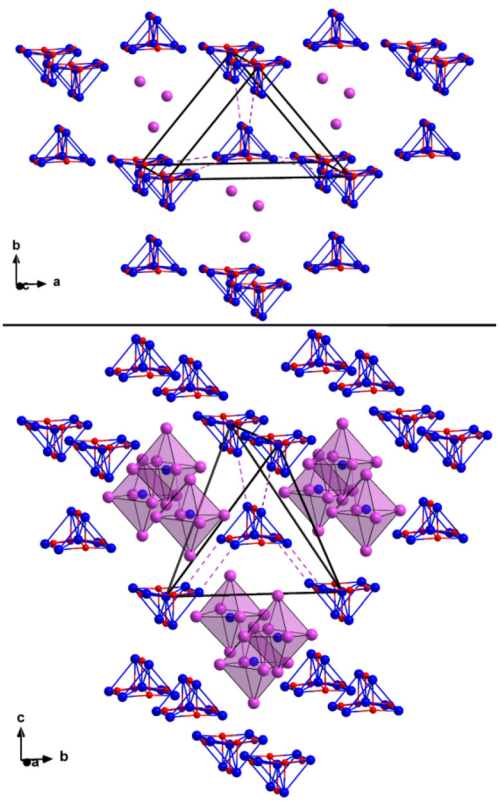

Fig. 6 Comparison of the cluster arrangement in $Li_3Nb_7O_5I_{15}$ (top) and $Li_3Nb_7O_5I_{14}(NbI_6)$ (bottom) with the created cavities for I^- (violet balls) and $(NbI_6)^-$ ions (violet polyhedra). Two iodide bridges, which connect the central cluster with six and four adjacent clusters, respectively, are illustrated with pink dashed lines.

For $Li_3Nb_7O_5I_{15}$, this results in a structural arrangement where each $[Nb_7O_5]$ cluster is surrounded by six adjacent clusters *via* iodine bridges. In contrast, in $Li_3Nb_7O_5I_{14}(NbI_6)$, the $[Nb_7O_5]$ cluster core connects only to four adjacent clusters *via* iodine bridges.

Conclusion

The series of previously known metal-rich niobium oxyiodides is complemented by the basic compound $Li_3Nb_7O_5I_{14}(NbI_6)$, which appears as a major phase at 450 °C, but is transformed at slightly higher temperatures into other newly discovered niobium oxyiodide compounds. The crystal structures of $Li_3Nb_7O_5I_{14}(NbI_6)$ and $Li_3Nb_7O_5I_{15}$ show a close structural relationship to each other, and both phases appear as bottom phases in the reaction vessel, compared to other compounds in this system.

The discovery of the large series of compounds and crystal structures arises from the heterogeneous reaction between NbI_4 and Li_2O, with $Li_2(CN_2)$ serving as a mild reduction agent. These reaction conditions permit niobium, oxygen, and iodine to coexist as gas phase species (*e.g.* as NbI_x, $NbOI_2$, I_2, *etc.*). The composition of the gas phase is thought to be decisive for the formation of multiple compounds in one and the same reaction, allowing formation conditions for several phases, possibly under locally marginal temperature and pressure gradients, or cooling rates, as would be likely expected for non-equilibrium conditions. This finding and recent developments in the field of niobium oxyiodides expand the knowledge beyond the previously reported compounds $NbOI_3$, NbO_2I and $NbOI_2$ by the newly reported examples Nb_4OI_{10}, Nb_4OI_{11} (two modifications), Nb_4OI_{12}, $Nb_5O_4I_{11}$, $Li_3Nb_7O_5I_{15}$, $Nb_6O_3I_{15}$, $Nb_8O_5I_{17}(NbI_5)$, $Nb_{11}O_6I_{24}$, and $Li_3Nb_7O_5I_{14}(NbI_6)$. Some of these metal-rich compounds have been reported to exhibit semiconducting behaviour, although in practice their applications are limited by their moisture sensitivity, which is characteristic for all reported niobium oxyiodides.

Experimental section

All manipulations of starting materials and products were performed in a glovebox under dry argon with moisture and oxygen levels below 1 ppm. Li_2O (ABCR, 95%) was used as purchased. NbI_4 was synthesised as described in the literature.[24] $Li_2(CN_2)$ was synthesised as described before.[16]

Synthesis of $Li_3Nb_7O_5I_{14}(NbI_6)$

$Li_3Nb_7O_5I_{14}(NbI_6)$ was synthesised from NbI_4, Li_2O and $Li_2(CN_2)$. For this purpose, NbI_4 (160.8 mg, 0.268 mmol), Li_2O (2 mg, 0.067 mmol) and $Li_2(CN_2)$ (7.2 mg, 0.135 mmol) were encapsulated into a fused and evacuated silica ampoule with a length of 3 cm and a volume of about 1.5 cm^3. The ampoule was heated in a box furnace from room temperature to 450 °C

at a rate of 0.1 °C min^{-1}. The holding time was 24 h before the reaction mixture was cooled to room temperature at a rate of 10 °C min^{-1}. A block like, polycrystalline material of $Li_3Nb_7O_5I_{14}(NbI_6)$ was obtained at the bottom of the ampoule in the powder form, besides LiI and an amorphous phase, produced by the decomposition of $Li_2(CN_2)$. The product was washed with dry acetonitrile to remove coproduced LiI. The estimated yield of $Li_3Nb_7O_5I_{14}(NbI_6)$ was about 70%, intermingled with finely divided niobium powder, which is inappropriate for compositional chemical analysis. The crystalline powder appears black and decomposes in moist air.

Powder X-ray diffraction

PXRD patterns of products were obtained using a Stadi-P (STOE, Darmstadt) powder diffractometer with germanium monochromated Cu-$K_{\alpha1}$ radiation (λ = 1.5406 Å) and a Mythen 1K detector.

Conflicts of interest

The authors declare no conflicts of interest.

Data availability

Crystallographic data have been deposited at the CCDC under 2493985.[25] The data that support the findings of this study are available on request from the corresponding author, H.-J. Meyer.

Acknowledgements

Funding by the Deutsche Forschungsgemeinschaft through grant ME 914/32-1 is gratefully acknowledged.

References

1 A. Simon, H.-G. von Schnering and H. Schäfer, *Z. Anorg. Allg. Chem.*, 1967, **355**, 295–310.
2 A. Simon and H.-G. von Schnering, *J. Less-Common Met.*, 1966, **11**, 31–46.
3 P. W. Seabaugh and J. D. Corbett, *Inorg. Chem.*, 1965, **4**, 176–181; L. F. Dahl and D. L. Wampler, *Acta Crystallogr.*, 1962, **15**, 903–911.
4 H.-J. Meyer and J. D. Corbett, *Inorg. Chem.*, 1991, **30**, 963–967; H.-J. Meyer, *Z. Anorg. Allg. Chem.*, 1994, **620**, 863–866; F. Grahlow, F. Strauß, M. Scheele, M. Ströbele, A. Carta, S. F. Weber, S. Kroeker, C. P. Romao and H.-J. Meyer, *Phys. Chem. Chem. Phys.*, 2024, **26**, 11789–11797.
5 M. D. Smith and G. J. Miller, *J. Alloys Compd.*, 1998, **281**, 202–205.
6 H. B. Yaich, J. C. Jegaden, M. Potel, M. Sergent, A. K. Rastogi and R. Tournier, *J. Less-Common Met.*, 1984, **102**, 9–22.
7 G. J. Miller and J. Lin, *Angew. Chem., Int. Ed. Engl.*, 1994, **33**, 334–336.
8 M. Ströbele, O. Oeckler, M. Thelen, R. F. Fink, A. Krishnamurthy, S. Kroeker and H.-J. Meyer, *Inorg. Chem.*, 2022, **61**, 17599–17608.
9 J. Rijnsdorp and F. Jellinek, *J. Less-Common Met.*, 1978, **61**, 79–82; S. Hartwig and H. Hillebrecht, *Z. Naturforsch.*, 2007, **62**, 1543–1548; S. Hartwig and H. Hillebrecht, *Z. Anorg. Allg. Chem.*, 2007, **634**, 115–120.
10 L. Pan, Y.-L. Wan, Z.-Q. Wang, H.-Y. Geng and X.-R. Chen, *J. Appl. Phys.*, 2023, **134**, 085105.
11 Y. Jia, M. Zhao, G. Gou, X. C. Zeng and J. Li, *Nanoscale Horiz.*, 2019, **4**, 1113–1123.
12 C. Liu, X. Zhang, X. Wang, Z. Wang, I. Abdelwahab, I. Verzhbitskiy, Y. Shao, G. Eda, W. Sun, L. Shen and K. P. Loh, *ACS Nano*, 2023, **17**, 7170–7179.
13 V. Kolesnichenko, D. C. Swenson and L. Messerle, *Inorg. Chem.*, 1998, **37**, 3257–3262.
14 M. Ströbele, A. Mos and H.-J. Meyer, *Inorg. Chem.*, 2013, **52**, 6951–6956; A. Mos, M. Ströbele and H.-J. Meyer, *Z. Anorg. Allg. Chem.*, 2015, **641**, 1722–1727; A. Mos, M. Ströbele and H.-J. Meyer, *J. Cluster Sci.*, 2015, **26**, 187–198.
15 A. Mos, C. Castro, S. Indris, M. Ströbele, R. F. Fink and H.-J. Meyer, *Inorg. Chem.*, 2015, **54**, 9826–9832.
16 R. Srinivasan, M. Ströbele and H.-J. Meyer, *Inorg. Chem.*, 2003, **42**, 3406–3411.
17 K. Gibson, M. Ströbele, B. Blaschkowski, J. Glaser, M. Weisser, R. Srinivasan, H. J. Kolb and H.-J. Meyer, *Z. Anorg. Allg. Chem.*, 2003, **629**, 1863–1870.
18 J. Beitlberger, M. Ströbele, P. Schmidt, C. P. Romao and H.-J. Meyer, *Dalton Trans.*, 2025, **54**, 14376–14383.
19 J. Beitlberger, M. Ströbele, F. Strauß, M. Scheele, C. P. Romao and H.-J. Meyer, *Eur. J. Inorg. Chem.*, 2024, **27**, e202400329; J. Beitlberger, M. Martin, M. Scheele, P. Schmidt, M. Ströbele and H.-J. Meyer, *Dalton Trans.*, 2025, **54**, 5486–5493.
20 F. Grahlow, J. Beitlberger, M. Martin, E. Juriatti, H. Peisert, M. Scheele, M. Ströbele, C. P. Romao and H.-J. Meyer, *Dalton Trans.*, 2025, **54**, 16593–16604.
21 J. Beitlberger, M. Martin, M. Scheele, M. Matas, C. P. Romao, M. Ströbele and H.-J. Meyer, *arXiv*, 2026, preprint, arXiv:0262.16011, DOI: 10.48550/arXiv:2602.16011.
22 H. Schäfer and H.-G. von Schnering, *Angew. Chem.*, 1964, **76**, 833–849; A. Simon, H.-G. von Schnering, H. Wöhrle and H. Schäfer, *Z. Anorg. Allg. Chem.*, 1965, **339**, 155–170; B. Baján and H.-J. Meyer, *Z. Naturforsch.*, 1995, **50**, 1373–1376.
23 K. Habermehl, A.-V. Mudring and G. Meyer, *Eur. J. Inorg. Chem.*, 2010, **2010**, 4075–4078.
24 G. Brauer, *Handbuch der präparativen anorganischen Chemie*, Enke, 1975.
25 CCDC 2493985: Experimental Crystal Structure Determination, 2026, DOI: 10.25505/fiz.icsd.cc2pq64s.